Journal of Catalysis 260 (2008) 141–149

Contents lists available at ScienceDirect

Journal of Catalysis

www.elsevier.com/locate/jcat

Effects of alkali additives on the physicochemical characteristics and chemisorptive properties of Pt/TiO_2 catalysts

Paraskevi Panagiotopoulou, Dimitris I. Kondarides [*]

Department of Chemical Engineering, University of Patras, GR-26504 Patras, Greece

ARTICLE INFO

Article history:
Received 9 June 2008
Revised 23 August 2008
Accepted 21 September 2008
Available online 16 October 2008

Keywords:
Platinum
Titanium dioxide
Promotion
Alkali
Cesium
Sodium
Hydrogen
Carbon monoxide
TPD
TPR
DRIFTS
FTIR

ABSTRACT

The effects of alkali additives on the physicochemical and chemisorptive properties of 0.5% Pt/TiO_2 have been investigated over catalysts promoted with variable amounts of Na (0–0.2 wt%) or Cs (0–0.68 wt%) with the use of diffuse reflectance infrared spectroscopy (DRIFTS) and temperature-programmed (TPD, TPR) techniques. It has been found that addition of alkalis does not affect adsorption of CO and H_2 on the surface of Pt crystallites, indicating the absence of strong electronic-type interactions between these sites and the promoters. However, the presence of alkalis results in the creation and population of new sites with increased electron density, proposed to be located at perimetric sites of Pt crystallites, which are in contact with the support. The adsorption strength of these sites toward CO increases with increasing alkali content, which is evidenced by the development of new, low-frequency IR bands in the ν(CO) region. In contrast, addition of alkali results in weakening of hydrogen adsorption on sites located at the metal/support interface, which is reflected to a significant shift of the corresponding TPD peak toward lower temperatures. Results of CO-TPD experiments indicate that CO adsorbed on Pt interacts with hydroxyl groups associated with the support to yield formate, which decomposes during TPD to CO_2 and H_2. Thermal decomposition of formate is accomplished at lower temperatures in the presence of alkali. Finally, CO-TPR experiments indicate that the reducibility of TiO_2 is enhanced in the presence of alkali, which can be related to the creation of the new sites at the metal/support interface.

1. Introduction

Electropositive promoters, such as alkali and alkaline earth metals, are frequently used as additives in heterogeneous catalysis in order to improve catalytic activity, selectivity and/or durability. Well known examples of industrially important catalytic reactions promoted by alkalis are the Fischer–Tropsch synthesis of hydrocarbons and the ammonia synthesis from N_2 and H_2 [1]. In recent years, significant efforts have been made to modify catalytic performance of noble metal catalysts by chemical [2–12] or electrochemical [13–15] promotion with alkali metals, in order to change product distribution, to reduce the energy requirements (reaction temperature) or to decrease the amount of precious metal required for a specific reaction to occur. In most cases, it has been found that addition of alkalis results in a significant improvement of catalytic performance and that the promotional effect, which often depends on the size of the dopant atom, is maximized for a certain alkali content on the catalytic surface [2–15].

The ability of alkali additives to modify catalytic activity and/or selectivity can be understood by considering the effects induced by the promoting species on the chemisorptive properties of metal surfaces toward reactive molecules. These effects may originate from either electronic interactions, i.e., modification of electron density of alkali-promoted metal surfaces, and/or from electrostatic interactions associated with alkali-metal ions, and/or from site blockage [16–18]. Regarding the electronic-type effects, alkali metals are electron donors and, therefore, may act by enhancing chemisorption of electron acceptor species, such as carbon monoxide and oxygen, and/or by suppressing chemisorption of electron donors, such as olefins and hydrogen [13]. These issues have been investigated extensively in recent years, mainly with the use of carbon monoxide as probe molecule. Several fundamental studies conducted over single crystals of transition metals [17,19] and noble metals [17,18,20] have shown that the presence of alkali-metal atoms modifies adsorption characteristics of the metal surface toward CO leading to: (a) a dramatic increase in the binding energy of CO (strengthening of the metal–CO bond), which is reflected to the large shift in desorption temperature in TPD experiments, (b) a significant weakening of the carbon–oxygen bond, which is evidenced by the marked decrease in the frequency of the C–O stretch vibration, and (c) a shift in the electron binding energies of both core and valence levels. Qualitatively similar results have been obtained for alkali-promoted noble metal catalysts supported on SiO_2 [21–23], Al_2O_3 [8,24] or zeolite [25]. Additional effects of alkalis on

---

[*] Corresponding author. Fax: +30 2610 991527.
E-mail address: dimi@chemeng.upatras.gr (D.I. Kondarides).

0021-9517/$ – see front matter
doi:10.1016/j.jcat.2008.09.014

Table 1
Physicochemical characteristics of alkali-promoted 0.5% Pt/TiO_2 catalysts.

Promoter type and nominal loading (wt%)		Alkali:Pt atomic ratio (nominal)	SSA[a] ($m^2\ g^{-1}$)	Surface alkali concentration ($atom\ nm^{-2}$)	Anatase content[b] (%)	Platinum dispersion[c]	d_{Pt}[d] (Å)
None	0	0.0	29	0	48	0.87	12
Na	0.017	0.3	30	0.15	52	0.94	11
	0.06	1.0	27	0.58	56	1.01	10
	0.12	2.0	28	1.1	50	0.66	15
	0.20	3.4	28	1.9	56	0.81	13
Cs	0.17	0.5	30	0.26	50	0.78	13
	0.34	1.0	28	0.55	48	0.77	13
	0.68	2.0	28	1.1	59	0.74	14

[a] Specific surface area, estimated with the BET method.
[b] TiO_2 phase composition estimated from integral intensities of the anatase (101) and rutile (110) XRD reflections.
[c] Estimated from selective chemisorption of CO at room temperature.
[d] Mean crystallite size of dispersed Pt crystallites.

the properties of supported metal catalysts include modification of the acid/base characteristics of the support [4,11,12] and inhibition of spillover of adsorbed species [6,23].

The present investigation was undertaken in order to develop an understanding of the effects of alkali promotion on the physicochemical and chemisorptive properties of Pt/TiO_2 catalysts, which have been found to be very active for the low-temperature water–gas shift (WGS) reaction [26–29]. Results of the present study provide the basis for explaining the enhanced WGS activity of alkali-promoted Pt/TiO_2 catalysts, which will be discussed in a forthcoming publication.

2. Experimental

2.1. Catalyst preparation and characterization

Alkali-promoted TiO_2 carriers were prepared by impregnation of titanium dioxide powder (Degussa P25) with an aqueous solution of the corresponding alkali precursor salt ($NaNO_3$, $CsNO_3$). Typically, 5 g of TiO_2 were added under continuous stirring in 50 mL of water containing the desired amount of the salt, at natural solution pH. The resulting slurry was heated slowly at 70 °C under continuous stirring and maintained at that temperature until nearly all the water evaporated. The solid residue was dried at 110 °C for 24 h and subsequently calcined in air at 600 °C for 3 h. The promoter concentration of samples thus prepared varied in the ranges of 0–0.20 wt% (0–1.9 $atoms\ nm^{-2}$) and 0–0.68 wt% (0–1.1 $atoms\ nm^{-2}$) for Na and Cs dopants, respectively (Table 1).

Dispersed platinum catalysts (0.5 wt% Pt) were prepared employing the wet impregnation method with the use of the above carriers and $(NH_3)_2Pt(NO_2)_2$ (Alfa) as platinum precursor salt. Materials were characterized with respect to their specific surface area, anatase content, primary crystallite size of TiO_2 and Pt dispersion, employing nitrogen physisorption at the temperature of liquid nitrogen (BET method), X-ray diffraction (XRD) and selective chemisorption of CO at room temperature. Details on the equipment and procedures used for catalyst preparation and characterization can be found elsewhere [26].

2.2. In situ FTIR spectroscopy

Fourier transform infrared (FTIR) experiments were carried out using a Nicolet 740 FTIR spectrometer equipped with a diffuse reflectance (DRIFT) cell (Spectra Tech), an MCTB detector and a KBr beam splitter. The cell is directly connected to a flow system, equipped with mass flow controllers and a set of valves which allow control of feed gas composition [28]. In a typical experiment, the catalyst powder was heated at 450 °C under He flow for 10 min and then reduced in flowing hydrogen (20% H_2 in He) at 300 °C for 60 min. The reduced sample was flushed with He at 450 °C for 10 min and subsequently cooled down to room temperature (RT). During the cooling stage, background spectra were collected at temperatures of interest. The flow was then switched to a gas mixture of 1% CO in He at RT for 30 min. Finally, the system was purged with He for 10 min and temperature was stepwise increased up to 450 °C. Spectra were recorded 3 min after reaching the desired temperature. In all experiments, the total flow through the DRIFT cell was 30 cm^3/min.

2.3. Temperature-programmed desorption of H_2 or CO

Temperature-programmed desorption (TPD) experiments were carried out using an apparatus and following the procedures described in detail elsewhere [30]. In a typical experiment, an amount of 200 mg of freshly prepared catalyst ($0.18 < d < 0.25$ mm) was placed in a quartz microreactor, heated at 500 °C under He flow for 15 min and then reduced *in situ* at 300 °C for 30 min under flowing hydrogen. The catalyst was heated again at 500 °C under He flow for 15 min, in order to remove adsorbed species from the catalyst surface, and then cooled down to 25 °C. The flow was then switched to the adsorbing gas, H_2 or CO (1% in He), for 15 min, followed by purging with He for 10 min at RT. After this step, temperature was increased linearly ($\beta = 30\,°C/min$) up to 650 °C and TPD patterns were recorded with the use of a mass spectrometer (Fisons, SXP Elite 300H) connected on-line to the reactor outlet. Responses of the mass spectrometer were calibrated against standard mixtures of accurately known composition. When necessary (e.g. CO_2–CO signals), the cracking coefficient determined in separate experiments was also taken into account in the calculations of gas effluent concentrations.

2.4. Temperature-programmed reduction experiments

Temperature-programmed reduction (TPR) experiments were carried out using carbon monoxide (CO-TPR) as reducing agent, following the procedure described elsewhere [26]. In a typical experiment, 200 mg of the catalyst were placed in a quartz microreactor and treated at 300 °C with a flowing 2% O_2/He mixture for 30 min. The sample was then heated under He flow at 500 °C for 15 min and subsequently cooled down to room temperature. TPR experiments were then carried out over the pre-oxidized samples by switching the feed composition from He to 0.25% CO/He (40 cm^3/min), left at 25 °C for 10 min, and then heating linearly ($\beta = 30\,°C/min$) at 650 °C. A mass spectrometer (Omnistar/Pfeiffer Vacuum) was used for on-line monitoring of TPR effluent gas. The transient-MS signals at $m/z = 2$ (H_2), 15 (CH_4), 18 (H_2O), 28 (CO)

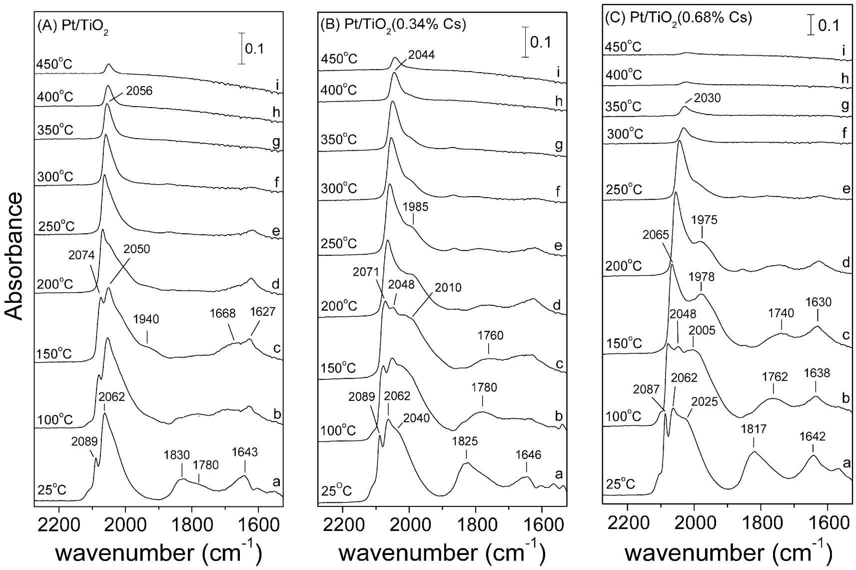

Fig. 1. DRIFT spectra obtained from (A) Pt/TiO$_2$ (unpromoted), (B) Pt/TiO$_2$ (0.34 wt% Cs) and (C) Pt/TiO$_2$ (0.68 wt% Cs) catalysts following adsorption of CO at 25 °C for 30 min and subsequent stepwise heating at the indicated temperatures under He flow.

and 44 (CO$_2$) were continuously recorded. Determination of cracking coefficients and calibration of the mass spectrometer signals were made as described above (Section 2.3).

3. Results and discussion

3.1. Physicochemical characteristics of synthesized catalysts

Results of physicochemical characterization of the synthesized materials are summarized in Table 1, where the specific surface area (SSA), TiO$_2$ phase composition (% anatase), platinum dispersion and average size of Pt crystallites (d_{Pt}) are listed as functions of promoter type and nominal loading. Regarding the unpromoted catalyst, it is observed that the values of both SSA (29 m^2/g) and anatase content (48%) are substantially lower, compared to those of the parent TiO$_2$ material (48 m^2/g, 75% anatase). This is because synthesis of all catalyst samples included heat treatment at elevated temperature (600 °C for 3 h), which is known to result in transformation of TiO$_2$ to its rutile form, particle growth and decrease of specific surface area [31]. Addition of alkalis does not affect, practically, SSA but leads to materials with higher anatase content, compared to the undoped sample (Table 1). The mean primary crystallite size of TiO$_2$, estimated from X-ray line broadening [26], is not affected significantly by the presence of the promoters and varies in the range of 20–26 nm for all catalyst samples investigated. Results of CO chemisorption measurements show that platinum is well dispersed for all catalyst samples, with the average size of Pt crystallites ranging between 1.0 and 1.5 nm (Table 1).

3.2. FTIR investigation of CO adsorption/desorption characteristics

In Fig. 1A are shown DRIFT spectra obtained from the unpromoted Pt/TiO$_2$ catalyst following exposure to 1% CO/He at 25 °C for 30 min and subsequent stepwise heating at 450 °C under He flow. It is observed that the spectrum recorded at 25 °C (trace a) is characterized by bands in the ν(CO) stretching frequency region, located at 2089, 2062, 1830 and 1780(sh) cm^{-1}. Additional bands located below 1700 cm^{-1} (not all of them shown for clarity) are due to formate and/or carbonate species associated with the support [28]. The band at 2089 cm^{-1} is often attributed to linear CO adsorbed on partially oxidized platinum sites (Pt$^{\delta+}$) [28,32], but this is probably not the case here because the catalyst was reduced *in situ* with hydrogen at 300 °C prior to exposure to CO. Therefore, the bands at 2089 and 2062 cm^{-1} can be assigned to CO linearly adsorbed on Pt terrace and step sites, respectively [33,34]. The band at 1830 cm^{-1} is characteristic of bridge-bonded CO on reduced platinum sites [28,32,35] whereas its low frequency shoulder, located at ca. 1780 cm^{-1}, has been assigned to 3-fold bridged CO species [36]. As will be discussed below, this band can be attributed to bridged CO species adsorbed at the metal/support interface. Stepwise heating from 25 to 450 °C under He flow results in the disappearance of bands attributed to bridged CO above 150 °C and to a progressive decrease of the intensities of linear Pt–CO bands (traces a–i). This is accompanied by a shift of linear CO bands toward lower wavenumbers, which is consistent with a decrease of the vibrational coupling of adjacent CO dipoles with decreasing coverage [28,32,35].

It is of interest to note that a new band, located at ca. 1940 cm^{-1}, is resolved in the temperature range of 100–200 °C (traces b–d). The low frequency of this band, which cannot be solely explained by a decrease in dipole–dipole coupling (e.g., adsorption on isolated platinum sites), indicates the presence of adsorption sites of exceptional electron-donating properties. Similar bands, located in the region of 1940–1980 cm^{-1}, have been reported for a number of noble metal catalysts dispersed on reducible supports, including Pt/TiO$_2$ [28,35], Au/TiO$_2$ [37], Pt/CeO$_2$ [36,38] and Pd/CeO$_2$ [39], and were assigned to CO adsorption on metal sites strongly interacting with the metal oxide support. In our previous study [28], the band observed in this frequency region has been tentatively assigned to terminal CO species adsorbed on metallic Pt in contact with Ti^{3+} ions. Such [Pt-Ti^{3+}] sites are expected to be present at the metal–support interface under reducing conditions. The appearance of the 1940 cm^{-1} band upon thermal treatment implies that population of [Pt-Ti^{3+}] sites has an activation energy barrier to CO adsorption, which may be related to reduction of the titania surface. In particular, it may be suggested that thermal treatment of Pt/TiO$_2$ catalysts in the presence of adsorbed CO results in partial reduction of TiO$_2$ in the vicinity of Pt crystallites and, concomitantly, in the creation and population of the so formed [Pt-Ti^{3+}] sites. If this is the case, then the observed activation energy barrier for CO adsorption should be due to partial reduction of TiO$_2$ and thermal generation of [Pt-Ti^{3+}] sites at the metal/support interface.

In Fig. 1B are presented DRIFT spectra obtained over Pt/TiO_2 catalyst promoted with 0.34% Cs. The spectrum recorded at 25 °C (trace a) consists of bands corresponding to linear (2089, 2062 cm^{-1}) and bridged (1825 cm^{-1}) CO species, similar to those discussed above for the unpromoted catalyst. However, comparison of spectra obtained for the two samples shows the following important differences: First, the bridge-to-linear band intensity ratio (B:L ratio) is considerably higher for the Cs-promoted catalyst. Second, an additional low frequency (LF) band, located at ca. 2040 cm^{-1}, is discernible over the alkali-modified sample, which shifts toward lower frequencies with increasing temperature (traces a–i). This shift seems to be accompanied by a transfer of intensity from the CO band at 2062 cm^{-1}, which implies redistribution of adsorbed CO species with increasing temperature. A similar effect of temperature is observed for the bridged CO band, the maximum of which shifts from 1825 cm^{-1} at 25 °C to ca. 1760 cm^{-1} at 200 °C (traces a–d). This seems to be due to the presence a new, LF-bridged CO band, which develops and shifts toward lower wavenumbers in a way similar to that discussed above for the LF-linear CO band.

Increasing Cs content to 0.68% (Fig. 1C) does not affect the positions of linear CO bands at 25 °C, relative to those observed for the unmodified catalyst (2087 and 2062 cm^{-1}), but results in a further (although smaller) increase of the B:L ratio and in a red shift of the bridged-CO band maximum, which now appears at 1817 cm^{-1} (trace a). The LF-linear CO band observed at ca. 2040 cm^{-1} for the sample doped with 0.34% Cs appears now at lower wavenumbers (2025 cm^{-1}) and is of higher relative intensity. Increasing temperature results in a significant red shift of the low-frequency bands at 2025 cm^{-1} and 1817 cm^{-1} by ca. 50 cm^{-1} and 80 cm^{-1}, respectively (traces a–i). Again, the LF-linear CO band at 2025 cm^{-1} seems to develop at the expense of the band at 2062 cm^{-1} with increasing temperature.

Similar FTIR spectra were obtained for all alkali-promoted Pt/TiO_2 catalysts listed in Table 1, and representative results obtained for Na-containing samples are shown in Fig. 2. It is observed that modification of catalysts by sodium affects CO adsorption/desorption properties of Pt toward CO in a manner which is qualitatively similar to that discussed above for Cs-containing samples. The effects of alkali-promotion on the spectral characteristics of adsorbed CO can be summarized as follows: (i) adsorption of CO at room temperature (RT) results in all cases in the development of bands attributable to CO linearly adsorbed on Pt terrace (2089 cm^{-1}) and step (2062 cm^{-1}) sites. The positions of these bands at RT are not affected by the presence of alkali. These linearly adsorbed CO species are thermally very stable and, under the present experimental conditions, the corresponding bands disappear from the spectrum at temperatures typically higher than 400 °C; (ii) the band assigned to bridge-bonded CO, which is located at 1830 cm^{-1} for the unpromoted catalyst, increases in intensity and shifts toward lower frequencies in the presence of alkali. Both the B:L ratio and the extent of the red shift increase with increasing dopant content. Bridge-bonded CO species are thermally less stable than linear CO species and the corresponding bands disappear from the spectrum at temperatures in the range of 200–250 °C. Heat treatment results in a significant red shift of the bridged-CO band, by up to 80 cm^{-1}; (iii) addition of alkali metals results in the development of a new band in the $\nu(CO)$ region, which appears as a low-frequency shoulder of the linear CO bands. The band shifts toward lower frequencies and increases in intensity with increasing dopant concentration or temperature. The thermal stability of the corresponding species is intermediate to that of linear and bridged CO, and the band disappears from the spectrum at temperatures typically higher than 300 °C; (iv) careful inspection of FTIR spectra presented in Figs. 1–2 shows that the red shift of the bridged CO band discussed above is due to the development of a new LF-bridged CO band which is present in all spectra obtained over the alkali-promoted catalysts.

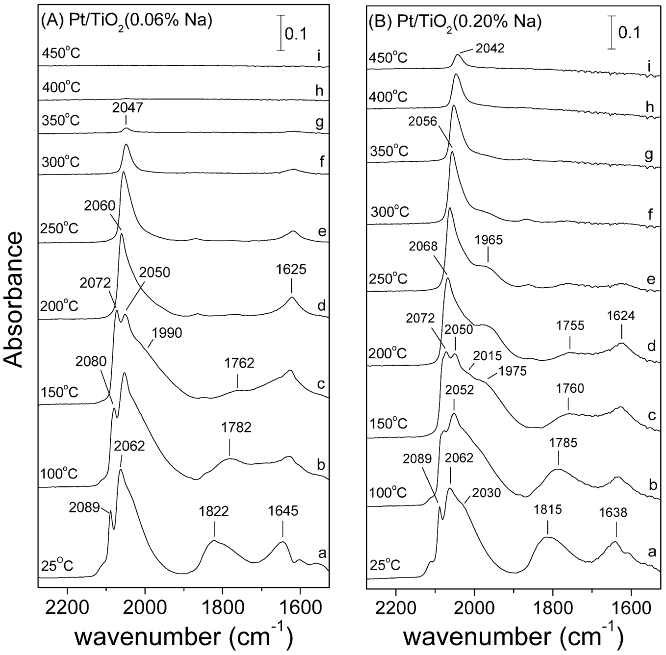

Fig. 2. DRIFT spectra obtained from Pt/TiO_2 catalysts promoted with (A) 0.06 wt% Na and (B) 0.20 wt% Na following adsorption of CO at 25 °C for 30 min and subsequent stepwise heating at the indicated temperatures under He flow.

The observed effects of the presence of alkali on the spectral characteristics of adsorbed CO can be understood by considering the influence of these promoters on the electronic and chemisorptive properties of dispersed platinum crystallites. Regarding the red shift observed for bands assigned to linear- and bridge-bonded CO, Primet [32] showed that the presence of electron donor compounds on the catalyst surface results in a substantial decrease of the $\nu(CO)$ stretching frequency due to electron transfer toward platinum, which increases the back-donation of the metal electrons into the $2\pi^*$ antibonding orbitals of adsorbed CO. Thus, alkali additives result in strengthening of the metal–CO (M–CO) bond and weakening of the carbon–oxygen (C–O) bond. Theoretical studies [40] have shown that increasing the electron density of a metal surface should also result in an increase of the integrated B:L intensity ratio, in agreement with the present results. A qualitatively similar behavior has been reported for a variety of alkali-modified noble metal catalysts, including Pt/SiO_2 [41], Pd/SiO_2 [23], Pt/ZrO_2 [9,10] and Pt/zeolite [41,42].

A very interesting characteristic of DRIFT spectra obtained at RT is that alkali loading does not affect, practically, the position of bands attributed to linear CO species adsorbed on terrace (2089 cm^{-1}) and step (2062 cm^{-1}) Pt sites (Figs. 1, 2). This indicates the absence of a strong electronic effect of the additives on the adsorption strength of these sites. In contrast, the positions and intensities of both the LF-linear and the LF-bridged CO bands depend on the nature and level of loading of the promoter. This implies that the species corresponding to the latter two bands are associated with adsorption sites, which are directly influenced by the presence of alkalis. It should be remembered here that dopants were added to TiO_2 carrier prior to deposition of platinum and, therefore, alkali atoms should be located mainly on the support rather than on the surface of Pt crystallites. This assumption is supported by results obtained over Cs-promoted Rh/Al_2O_3, where it was shown that Al_2O_3 support scavenges the alkali species present on the catalyst surface and hence the metal is left relatively unperturbed [8]. It is then reasonable to suggest that bands appearing in the presence of alkalis at 2040–2025 cm^{-1} and 1825–1815 cm^{-1} (positions refer to spectra obtained at RT) are related to species adsorbed at the metal–support interface, since these sites should be affected more strongly by promoter species located on the support. Thus, it is proposed that the new LF-linear band, which is clearly resolved in all spectra obtained over alkali-promoted catalysts (Figs. 1, 2), is due to a linear CO species adsorbed at the perimetric sites of Pt crystallites, which are in contact with the support. The nature of these sites should be similar to that of [Pt-Ti^{3+}] sites discussed above for the unpromoted Pt/TiO_2 catalyst, because both refer to platinum sites of exceptionally high electron donating properties. Following the same reasoning, the LF-bridged CO band is attributed to bridge-bonded CO on the same sites. Inspection of spectra obtained at room temperature show that the presence of alkalis affects both the number (peak intensity) and electronic properties (peak position) of chemisorption sites located at the metal/support interface. The observed red shift of LF-CO bands with increase of alkali content can be understood by considering that increasing the number of alkali atoms in the vicinity of these sites results in increased electron transfer to platinum, whereas the increased intensity of IR bands can be related to the effects of the presence of alkali on the reducibility of TiO_2. These issues will be discussed in detail below, along with results of H_2-TPD and H_2-TPR experiments.

The observation that the LF-linear band develops with increasing temperature at the expense of the band assigned to linear CO on step Pt sites (2062 cm^{-1}) (Figs. 1, 2) indicates an increased interaction between Pt and the promoter species upon heating. The decreased intensity of the 2062-cm^{-1} band could be due to site blocking of step sites originating from migration of mobile promoter atoms from the support to the Pt crystallites with increasing temperature. It is also possible that this behavior is due to desorption and/or surface reaction of the corresponding species at lower temperature, compared to that of the unpromoted catalyst. Regarding the relatively large red shift of the LF-linear CO band upon heating, it can be attributed, at least in part, to interaction of the oxygen atom of CO adsorbed on perimetric sites of Pt crystallites with a Lewis acid site of the support (e.g., Pt-CO-Na^+, Pt-CO-Cs^+), which is expected to result in a decrease of the C–O bond order. This argument is in accordance with results reported in literature for alkali-modified Pd/SiO_2 [22,23] and Rh/SiO_2 [43] catalysts.

It should be noted here that, apart from the carbonyl bands discussed above, interaction of all catalysts investigated with CO resulted in the development of two "negative" bands in the ν(OH) region (not shown for clarity), located at ca. 3725 and 3670 cm^{-1}. In our previous study of unpromoted Pt/TiO_2 catalysts [28], it has been discussed in detail that the appearance of these bands is due to consumption of surface hydroxyl groups and indicates formation of surface formate species associated with the support. The absence of bands at around 2900 cm^{-1}, which are characteristic of formate, indicates that the population of this species is relatively low under the present experimental conditions. Thus, surface formate either decompose rapidly to yield hydrogen and CO_2 and/or is oxidized by surface oxygen atoms toward carbonate. Surface reactions related to the formation and fate of these species are discussed in detail below, along with results of CO-TPD experiments.

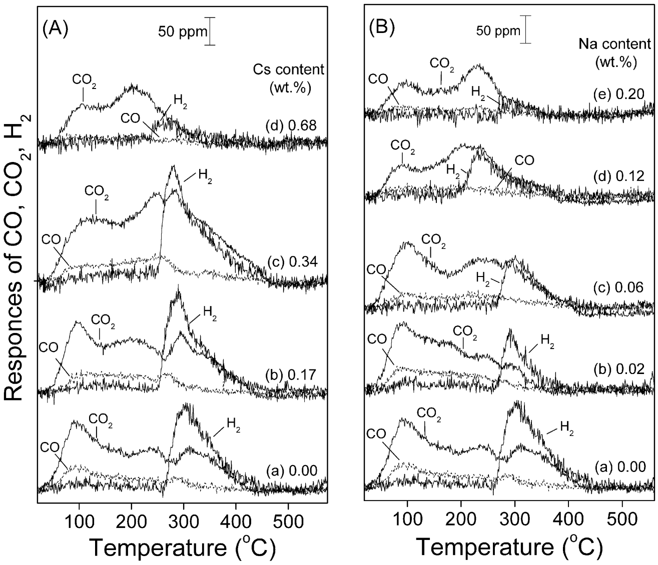

Fig. 3. Temperature-programmed desorption profiles obtained from Pt/TiO_2 catalysts doped with the indicated amounts of (A) cesium or (B) sodium promoters following exposure to 1% CO/He for 15 min at 25 °C. Experimental conditions: He flow: 30 $cm^3\,min^{-1}$; $\beta = 30\,°C\,min^{-1}$.

3.3. Temperature-programmed desorption of CO

TPD patterns obtained following interaction of the unpromoted and Cs-modified Pt/TiO_2 catalysts with CO at room temperature are shown in Fig. 3A. It is observed that CO desorbs from Pt/TiO_2 (profile a) in the temperature range of 50–350 °C, exhibiting two weak maxima located at ca. 100 °C and 290 °C. Desorption of CO is accompanied by evolution of CO_2 in the same temperature range, which is characterized by a low temperature (LT) peak at ca. 100 °C and a medium temperature (MT) peak at ca. 240 °C. An additional CO_2 peak, with its maximum located at ca. 315 °C, is observed at higher desorption temperatures. This high temperature (HT) CO_2 peak is accompanied by evolution of H_2 in the same temperature range. Comparison of the relative intensities of the CO and CO_2 TPD curves shows that only a small part of preadsorbed CO desorbs molecularly:

$$CO_{(Pt)} \rightleftarrows CO_{(g)}. \tag{1}$$

A significantly higher amount of adsorbed CO participates in surface reactions upon heating under He flow and yields CO_2 in the gas phase. Production of CO_2 may be attributed, at least in part, to reduction of surface TiO_2:

$$TiO_2 + xCO_{(Pt)} \rightarrow TiO_{2-x} + xCO_{2(g)} \quad (x < 2). \tag{2}$$

This is supported by results of our previous study [28] where it was clearly shown that, in the presence of dispersed Pt, CO (and also H_2) is able to reduce titania surface at relatively low temperatures. Another possible route for CO_2 production under the present experimental conditions is disproportionation of CO according to the Boudouard reaction:

$$2CO_{(Pt)} \rightarrow C + CO_{2\,(g)}. \tag{3}$$

The contribution of this reaction to the TPD response of CO_2 should not be significant for the unpromoted catalyst [44,45], but may be of importance for samples modified by alkalis. For instance, Pedrero et al. [6] found that CO_2 is produced over Cs-modified Pd/SiO_2 catalysts during contact with CO even at ambient temperatures via CO disproportionation promoted by Cs. Similar results have been reported for Na-promoted Pd/SiO_2 [23] and Ni/SiO_2 [46].

Regarding evolution of H_2 at high desorption temperatures, it should originate from interaction of adsorbed CO with hydroxyl groups associated with the support, i.e., the only possible source of hydrogen under the present experimental conditions. Thus, production of H_2 and CO_2 at temperatures higher than 250 °C can be attributed to the onset of the WGS reaction, which is believed to take place at the metal–support interface [28,44,45]:

$$CO_{(Pt)} + 2OH^-_{(TiO_2)} \rightarrow CO_{2(g)} + H_{2(g)} + O^{2-}_{(TiO_2)}. \tag{4}$$

Addition of small amounts of Cs on the catalyst surface results in significant changes in the TPD responses (Fig. 3A) and

Table 2
Amounts of species desorbed from the indicated Pt/TiO_2 catalysts in CO-TPD and H_2-TPD experiments.

Promoter type and nominal loading (wt%)		Amounts of species desorbed (μmol/g_{cat})			
		CO-TPD			H_2-TPD
		CO	CO_2	H_2	H_2
None	0	1.6	6.5	4.1	9.7
Na	0.017	2.2	6.3	2.3	8.1
	0.06	1.5	6.8	1.8	7.9
	0.12	1.1	4.6	2.0	8.2
	0.20	0.8	3.7	0.7	6.7
Cs	0.17	2.0	7.6	4.7	10.1
	0.34	2.7	11.2	5.5	12.2
	0.68	1.0	4.6	1.4	5.7

total amounts (Table 2) of desorbed CO, CO_2 and H_2 in a manner which depends on the level of doping. In particular, increasing Cs content from 0 to 0.34% (profiles a–c) does not affect significantly the position and intensity of the LT CO and CO_2 peaks but results in a progressive increase of the relative intensity of the MT CO_2 peak, which evolves in the temperature range of 150–270 °C. Comparison with FTIR spectra obtained over the same set of catalysts (Fig. 1) shows that the increased intensity of the MT CO_2 peak could be related to the development of the LF-linear band at 2040–1975 cm^{-1}, attributed to CO adsorbed at the metal/support interface. In particular, the relative population of this species increases with increasing Cs content to 0.34% and the corresponding band disappears from the spectrum at temperatures higher than 250 °C (Fig. 1B), i.e., in the same temperature range where evolution of the MT CO_2 peak is observed (Fig. 3A).

Increasing Cs content from 0 to 0.34% also results in an increase of the intensities of the HT CO_2 and H_2 peaks, which is accompanied by a progressive shift of their maxima toward lower temperatures, by ca. 35 °C (Fig. 3A, profiles a–c). However, further increase of Cs loading to 0.68% results in suppression of both HT CO_2 and H_2 peaks (profile d). These observations may be explained by considering that, as discussed above, evolution of CO_2 and H_2 at temperatures higher than ca. 250 °C originates from interaction of adsorbed CO with OH groups at the metal–support interface (Eq. (4)). This interaction results in the formation of surface formate species, which have been proposed to be active intermediates for the WGS reaction [47,48]:

$$CO_{(Pt)} + OH_{(TiO_2)} \rightarrow HCOO_{(Pt/TiO_2)}. \quad (5)$$

Formate species decompose with increasing temperature to yield hydrogen atoms adsorbed on platinum and CO_2, which either evolves in the gas phase or remains bonded to the support in the form of carbonates [28]:

$$HCOO_{(Pt/TiO_2)} \rightarrow H_{(Pt)} + CO_{2(TiO_2)}. \quad (6)$$

Finally, adsorbed hydrogen atoms and carbonates desorb from the catalyst surface to produce gas-phase H_2 and CO_2:

$$2H_{(Pt)} \rightarrow H_{2(g)}, \quad (7)$$

$$CO_{2(TiO_2)} \rightarrow CO_{2(g)}. \quad (8)$$

The increased amounts of HT CO_2 and H_2 observed for catalysts doped with 0.17% Cs (profile b) and 0.34% Cs (profile c), compared to those of unpromoted Pt/TiO_2 (profile a), can be attributed to the higher population of CO species adsorbed at the metal/support interface. This is supported by results of FTIR experiments (Fig. 1), which clearly show that increasing Cs content results in an increase of the relative population of CO species adsorbed at the periphery of Pt crystallites (band at 2040–1975 cm^{-1}). The alkali-induced increase of the population of this species should lead to formation of higher amounts of formate (Eq. (5)) which in turn leads to the production of higher amounts of H_2 and CO_2 in the gas phase (Eqs. (6)–(8)). The observed decrease of the amounts of HT CO_2 and H_2 evolved upon further increasing Cs content to 0.68% (profile d) may be attributed to dehydroxylation of the support, which is known to be caused by the presence of alkalis [6,23,49]. Thus, it may be argued that at sufficiently high Cs content, production of formate and, consequently, evolution of CO_2 and H_2 at temperatures higher than 250 °C is limited by the decreased population of hydroxyl groups.

Results of similar CO-TPD experiments obtained over Pt/TiO_2 catalysts doped with variable amounts of sodium are shown in Fig. 3B. It is observed that the effects of Na on the TPD pattern are qualitatively similar with those obtained for the Cs-doped catalysts and can be explained based on the same reasoning. In particular, increasing Na content results in: (a) an increase of the amount of CO_2 desorbed in the temperature range of ca. 150–270 °C (MT peak), (b) a progressive shift of the positions of the HT CO_2 and H_2 peaks toward lower desorption temperatures by ca. 60 °C (traces a–d), and (c) suppression of the amounts of CO_2 and H_2 desorbed above 250 °C at relatively high dopant levels (trace e). The obvious difference between TPD patterns obtained from Cs- and Na-doped samples is that in the former set of catalysts the amounts of CO_2 and H_2 desorbing above 250 °C (HT peaks) go through maxima with increasing dopant content, whereas in the latter set of catalysts the amounts of desorbed species in this temperature range decrease monotonically with increasing Na content. This behavior can be attributed to a different extent of dehydroxylation of the support induced by the two alkalis, which seems to be more significant for Na-doped catalysts even at low dopant levels. It should be noted, however, that the nominal surface concentration of added alkali (Table 1) is in most cases much lower than that of surface OH species of TiO_2 ($\sim 6\ nm^{-2}$).

Based on the above discussion, it is suggested that the amounts of HT CO_2 and H_2 desorbing at temperatures higher than 250 °C depend on the surface concentration of $HCOO_{(Pt/TiO_2)}$, which in turn depends on the population of adsorbed CO and hydroxyl groups at the metal–support interface. Regarding the shift of the HT CO_2 and H_2 peaks toward lower temperatures with increasing Cs (Fig. 3A) or Na (Fig. 3B) content, it may be related to the effect of dopants on the thermal stability of formate species formed at the metal–support interface (Eq. (6)). Pigos et al. have recently investigated the promoting effect of Na on the WGS activity of Pt/ZrO_2, in terms of the formate mechanistic perspective and found that addition of alkali influences the stability of surface formate [9,10]. In particular, it was shown that the presence of Na results in important weakening of the C–H bond, thereby promoting the rate of formate decomposition and favoring formation of carbonates, i.e., the precursor of gas-phase CO_2 [9,10]. This reasoning may explain the observed shift of the HT CO_2 and H_2 peaks toward lower temperatures with increasing Cs or Na content (Fig. 3).

3.4. *Temperature-programmed desorption of hydrogen*

Results of H_2-TPD experiments obtained following interaction of hydrogen with Na-promoted catalysts at 25 °C are shown in Fig. 4A. It is observed that the TPD curve recorded for the unpromoted sample (trace a) consists of a LT peak, located at ca. 115 °C, a MT peak, located at ca. 285 °C and a HT shoulder, located at ca. 350 °C. Addition of Na does not affect, practically, the position and intensity of the LT peak (traces b–e), indicating that adsorption/desorption characteristics of this species are not influenced appreciably by the presence of the promoter. In contrast, the MT peak shifts to progressively lower temperatures with increasing Na content, i.e., from ca. 285 °C for the undoped catalyst (trace a) to ca. 230 °C for the sample containing 0.20 wt% Na (trace e),

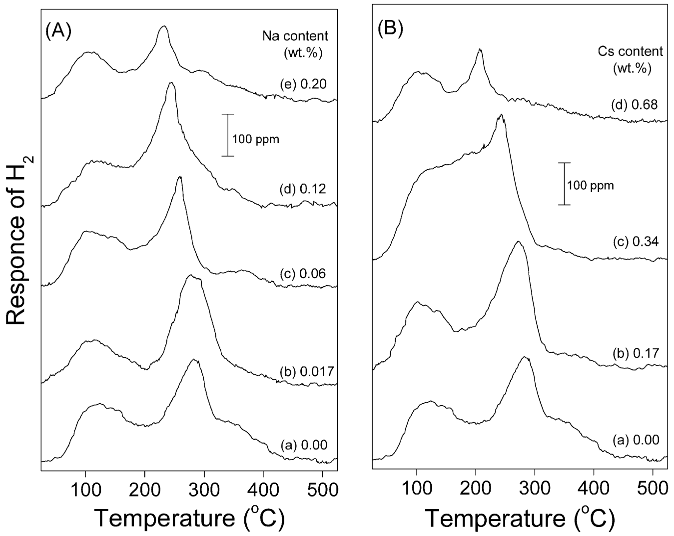

Fig. 4. Temperature-programmed desorption profiles obtained from Pt/TiO_2 catalysts doped with the indicated amounts of (A) sodium or (B) cesium promoters following adsorption of hydrogen at 25 °C for 15 min. Experimental conditions: same as in Fig. 3.

indicating a substantial weakening of the chemisorption bond of this species. Regarding the HT feature, which is clearly resolved over the unpromoted catalyst (trace a), it decreases in intensity with increasing Na content and is practically absent for samples containing 0.12–0.20 wt% Na (traces d–e). The total amount of desorbed hydrogen decreases from 9.7 $\mu mol\,g_{cat}^{-1}$ for the unpromoted catalyst to ca. 8.0 $\mu mol\,g_{cat}^{-1}$ for catalysts containing 0.017–0.12 wt% Na (Table 1). Further increase of Na content to 0.20 wt% results in a significant decrease of the amount of desorbed hydrogen to 6.7 $\mu mol\,g_{cat}^{-1}$, which is mainly due to the decrease of the MT peak (Fig. 4A).

Results of H_2-TPD experiments obtained over catalysts promoted with variable amounts of Cs are shown in Fig. 4B. As in the case of Na-promoted samples, the position and intensity of the LT peak do not change with increasing alkali content, whereas the maximum of the MT peak shifts significantly from 285 °C to 205 °C upon increasing Cs content from zero to 0.68 wt% (traces a–d). Addition of Cs also results in suppression of the HT feature, which is absent for samples containing more than 0.17 wt% Cs (traces c–d). Results summarized in Table 2 show that the total amount of desorbed hydrogen increases in the presence of small amounts of Cs (traces b, c), goes through a maximum for the sample containing 0.34 wt% Cs (trace c) and decreases significantly upon further increasing Cs content to 0.68 wt% (trace d).

The appearance of three desorption peaks in the H_2-TPD profiles of Fig. 4 indicates the presence of (at least) three states of adsorbed hydrogen species on the surface of alkali-promoted Pt/TiO_2 catalysts. The LT peak, which is generally observed over Pt single crystals [50,51] and supported platinum catalysts [52–55], can be assigned with certainty to hydrogen chemisorbed on the surface of dispersed metal crystallites. The observation that addition of Na or Cs does not result in appreciable changes of the desorption temperature or the intensity of the LT peak, implies that alkali promotion does not affect significantly the chemisorption strength or the population of hydrogen adsorbed on Pt crystallites, at least in the range of alkali concentrations used in the present study. It also provides additional evidence that alkali atoms are mainly located on the support and not on the surface of Pt crystallites. This behavior is in agreement with FTIR results of Figs. 1, 2, which also show that the stretching frequency and relative intensity of bands assigned to linearly adsorbed CO on Pt crystallites (bands at 2089 and 2062 cm^{-1}) are not affected by the presence of alkalis. Thus, results of both CO-FTIR and H_2-TPD experiments indicate that adsorption sites located on the surface of dispersed metal crystallites do not “feel” the presence of added alkali atoms.

Regarding the HT feature, which is clearly resolved in the TPD pattern obtained over the unpromoted catalyst (trace a), it can be related to desorption of spillover hydrogen. Generally, multiple TPD peaks observed at temperatures above ca. 300 °C are usually assigned to either spillover hydrogen, strongly chemisorbed hydrogen or hydrogen in subsurface layers of platinum [49,52,53]. Although other possibilities cannot be excluded, the present results indicate that the HT TPD peak is due to spillover hydrogen associated with the support. Formation of spillover hydrogen is generally enhanced with increasing adsorption temperature [53] and is inhibited for samples pretreated at elevated temperatures, due to partial dehydroxylation of the support [56]. Thus, the relatively low intensity of the HT peak obtained for Pt/TiO_2 (trace a) can be attributed to the high pretreatment temperature (600 °C) and/or the low adsorption temperature (25 °C) used in the present experiments. Assignment of the HT peak to spillover hydrogen is supported by the observation that addition of small amounts of alkali results in substantial decrease of the intensity of the HT peak, which disappears for higher dopant concentrations (Fig. 4). It is well known that the presence of alkali on metal oxide supports inhibits strongly hydrogen spillover [6,49].

The origin of the medium temperature H_2-TPD peak is of special interest, because both the chemisorption strength and the relative population of the corresponding species are affected drastically by the concentration of added alkali (Fig. 4). The desorption temperature of the MT peak is relatively low to be assigned to spillover hydrogen [49,52]. In addition, increasing alkali content does not result in a monotonic decrease and eventual disappearance of this peak, as would have been expected if alkali-induced dehydroxylation of the support was operable. Comparison with FTIR spectra of Figs. 1, 2 indicates that the MT H_2 peak can be related to the LF-CO bands, i.e., to CO adsorption on the only type of sites that depend strongly on the presence and concentration of added alkali. Thus, it is proposed that the MT H_2-TPD peak is due to hydrogen adsorbed at perimetric sites located at the metal/support interface. This assignment is in agreement with conclusions of previous work obtained over Pt/LTL zeolite [49] and supported Rh catalysts [57,58].

The downward shift of the MT-TPD peak with increasing Na (Fig. 4A) or Cs (Fig. 4B) content indicates a strong electronic type interaction between sites located at the metal/support interface and hydrogen. Weakening of the adsorption strength of these sites toward hydrogen implies that adsorption occurs following donation of electrons to platinum as has been reported, for example, for H_2 adsorption on K-doped iron catalysts [59]. If this is the case, then the presence of electron-donating alkali would be expected to result in weakening of the platinum–hydrogen bond, in agreement with results of Fig. 4. Thus, the effect of addition of alkali on the adsorption of hydrogen is opposite to that observed in the case of CO adsorption: alkali promotion results in strengthening of CO chemisorption but in weakening of hydrogen chemisorption on sites located the metal/support interface.

Weakening of the bond strength of hydrogen with increasing alkali content should be accompanied by a decrease of the population of this species. This does not seem to be the case here since the intensity of the MT-TPD peak tends to increase following addition of small amounts of alkali, which is more pronounced in the case of Cs-doped samples (Fig. 4B). This implies that addition of alkali may also result in the creation of new adsorption sites at the metal/support interface, as has been proposed by Marcelin et al. [60], who investigated adsorption of hydrogen over Cs- and Li-promoted Rh/TiO_2 catalysts. It may then be argued that

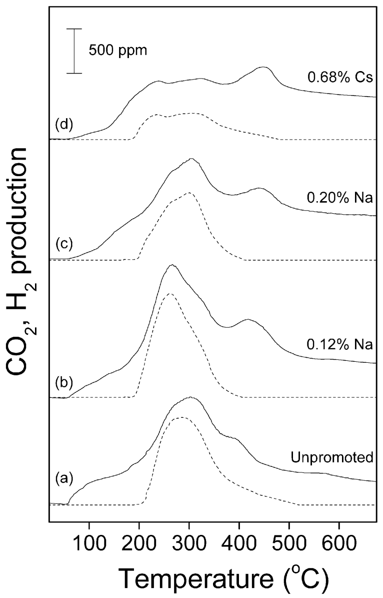

Fig. 5. Responses of CO_2 (solid lines) and H_2 (dashed lines) obtained during temperature-programmed reduction of the indicated preoxidized catalysts under flowing 0.25% CO/He mixture. Experimental conditions: total flow $= 40\ cm^3\,min^{-1}$; $\beta = 30\,°C\,min^{-1}$.

for low alkali content the population of hydrogen adsorbed at the metal/support interface increases due to the creation of new sites. However, for higher alkali concentrations the amount of hydrogen adsorbed decreases due to substantial weakening of the bond strength, which is the case for both Na- (Fig. 4A, trace e) and Cs-promoted (Fig. 4B, trace d) catalysts.

3.5. Temperature-programmed reduction with CO

The nature of the new sites created at the metal/support interface upon addition of alkali, could be similar to that of [Pt-Ti^{3+}] sites discussed above for the unpromoted Pt/TiO_2 catalyst, i.e., sites at the periphery of Pt crystallites, which are in contact with partially reduced titanium dioxide. In order to address this issue, the effect of alkali additives on the reducibility of Pt/TiO_2 catalysts has been investigated with temperature-programmed reduction (TPR) experiments carried out with the use of CO as the reducing agent. Results obtained over selected catalyst samples are shown in Fig. 5, where the responses of CO_2 and hydrogen produced during CO-TPR are plotted as functions of temperature. It is observed that CO_2 evolves from the unpromoted catalyst (profile a) in a wide temperature range, exhibiting three peaks centered at ca. 100, 300 and 400 °C. The MT CO_2 peak at 300 °C is accompanied by evolution of hydrogen in the same temperature range. As discussed in detail in our previous study [28], the LT peak centered at ca. 100 °C is due to reduction of platinum oxides (PtO_x) formed on the catalyst surface during the preoxidation step:

$$PtO_x + xCO \rightarrow Pt + xCO_2. \tag{9}$$

The MT CO_2 and H_2 peaks, located at ca. 300 °C, are due to the WGS reaction which, as discussed above, takes place at the metal/support interface between CO adsorbed on the metal and hydroxyl groups associated with the support (Eq. (4)). The HT shoulder observed at ca. 400 °C can be assigned to Pt-catalyzed, partial reduction of titanium dioxide (Eq. (2)).

Addition of Na (profiles b, c) or Cs (profile d) on the catalyst surface results in an increase of the intensity of the high temperature CO_2 peak, compared to that obtained over the unpromoted catalyst (profile a), indicating that abstraction of oxygen atoms from the TiO_2 support by CO (Eq. (2)) occurs more easily in the presence of alkali. In our previous study [28], it was clearly shown using Raman spectroscopy that the reducibility of titanium dioxide increases drastically with increasing specific surface area of the Pt/TiO_2 catalyst or, conversely, with decreasing primary particle size of TiO_2. Since materials used here have comparable SSA (Table 1) and primary crystallite size of TiO_2 (20–26 nm), the increased reducibility of the alkali-promoted catalysts should be attributed to the presence of dopants on the catalyst surface. This observation can be related with results of Krupay and Amenomiya [61], who studied chemisorption and oxygen exchange of CO and CO_2 on bare and K-promoted alumina. The authors concluded that potassium added onto alumina not only increases the number of exchangeable oxygen but also weakens the bonding of these oxygen atoms [61]. Since titanium dioxide is a reducible support, these effects should be more significant for TiO_2, compared to Al_2O_3, and could explain the enhanced reducibility of alkali-doped Pt/TiO_2 catalysts (Fig. 5). Clearly, a more detailed investigation is necessary to address these issues, which is beyond the scope of the present study.

4. Conclusions

Addition of small amounts of alkalis on the surface of a TiO_2 carrier results in significant modifications of the chemisorptive properties of dispersed Pt crystallites toward carbon monoxide and hydrogen. These effects are restricted to certain adsorption sites, and do not influence adsorption of CO or H_2 on the surface of Pt crystallites. In particular, addition of Na or Cs does not affect the position of IR bands related to CO adsorbed on terrace and step Pt sites but results in the development of new, low frequency bands attributed to species adsorbed on sites with increased electron-donating properties. It is proposed that these sites are located at the perimeter of Pt crystallites, which are in contact with the alkali-modified TiO_2 support. Increasing alkali content results in an increase of the relative population of these species and in strengthening of the Pt–CO bond, which is evidenced by the observed decrease in the C–O stretching frequency. These conclusions are supported by results of H_2-TPD experiments, which indicate that sites located at the surface of Pt crystallites do not “feel” the presence of added alkali. In contrast, the TPD peak attributed to hydrogen adsorbed at the metal/support interface, exhibits a significant shift toward lower temperatures with increasing Cs or Na content, indicating that the adsorption strength of these sites toward hydrogen decreases in the presence of electropositive alkali. Results of CO-TPD experiments provide evidence that CO adsorbed on Pt interacts with hydroxyl groups associated with the support to yield formate, which decompose during TPD to CO_2 and H_2. The population of surface formate depends on the level of doping, and its decomposition is accomplished at lower temperatures with increasing alkali content. Finally, CO-TPR experiments indicate that the reducibility of TiO_2 is enhanced in the presence of alkalis, thereby resulting in the creation of new adsorption sites at the metal/support interface.

References

[1] H.P. Bonzel, A.M. Bradshaw, G. Ertl (Eds.), Physics and Chemistry of Alkali Metal Adsorption, Elsevier, Amsterdam, 1989.
[2] I.V. Yentekakis, R.M. Lambert, M.S. Tikhov, M. Konsolakis, V. Kiousis, J. Catal. 176 (1998) 82.
[3] S.S. Mulla, N. Chen, L. Cumaranatunge, W.N. Delgass, W.S. Epling, F.H. Ribeiro, Catal. Today 114 (2006) 57.
[4] G. Avgouropoulos, E. Oikonomopoulos, D. Kanistras, T. Ioannides, Appl. Catal. B 65 (2006) 62.
[5] C. Kwak, T.-J. Park, D.J. Suh, Appl. Catal. A 278 (2005) 181.
[6] C. Pedrero, T. Waku, E. Iglesia, J. Catal. 233 (2005) 242.

[7] N. Iwasa, S. Arai, M. Arai, Appl. Catal. B 79 (2007) 132.
[8] D.G. Blackmond, J.A. Williams, S. Kesraoui, D.S. Blazewick, J. Catal. 101 (1986) 496.
[9] J.M. Pigos, C.J. Brooks, G. Jacobs, B.H. Davis, Appl. Catal. A 319 (2007) 47.
[10] J.M. Pigos, C.J. Brooks, G. Jacobs, B.H. Davis, Appl. Catal. A 328 (2007) 14.
[11] M.M. Telkar, C.V. Rode, V.H. Rane, R.V. Chaudhari, Catal. Commun. 6 (2005) 725.
[12] S.R. Demiguel, A.A. Castro, O.A. Scelza, J. Soria, Catal. Lett. 32 (1995) 281.
[13] C.G. Vayenas, S. Bebelis, C. Pliangos, S. Brosda, D. Tsiplakides, Electrochemical Activation of Catalysis, Kluwer Academic Publishers/Plenum Press, New York, 2001.
[14] O.A. Marina, I.V. Yentekakis, C.G. Vayenas, A. Palermo, R.M. Lambert, J. Catal. 166 (1997) 218.
[15] A. de Lucas-Consuegra, F. Dorado, J.L. Valverde, R. Karoum, P. Vernoux, J. Catal. 251 (2007) 474.
[16] J. Benzinger, R.J. Madix, Surf. Sci. 94 (1980) 119.
[17] D. Heskett, Surf. Sci. 199 (1988) 67.
[18] E.L. Garfunkel, J.E. Crowell, G.A. Somorjai, J. Phys. Chem. 86 (1982) 310.
[19] H.P. Bonzel, Surf. Sci. Rep. 8 (1987) 43.
[20] L.Q. Jiang, B.E. Koel, J.L. Falconer, Surf. Sci. 273 (1992) 273.
[21] V. Pitchon, M. Primet, H. Praliaud, Appl. Catal. 62 (1990) 317.
[22] P.A.J.M. Angevaare, H.A.C.M. Hendrickx, V. Ponec, J. Catal. 110 (1988) 11.
[23] L.F. Liotta, G.A. Martin, G. Deganello, J. Catal. 164 (1996) 322.
[24] S. Derrouiche, P. Gravejat, B. Bassou, D. Bianchi, Appl. Surf. Sci. 253 (2007) 5894.
[25] M.J. Kappers, J.T. Miller, D.C. Koningsberger, J. Phys. Chem. 100 (1996) 3227.
[26] P. Panagiotopoulou, D.I. Kondarides, J. Catal. 225 (2004) 327.
[27] P. Panagiotopoulou, D.I. Kondarides, Catal. Today 112 (2006) 49.
[28] P. Panagiotopoulou, A. Christodoulakis, D.I. Kondarides, S. Boghosian, J. Catal. 240 (2006) 114.
[29] P. Panagiotopoulou, D.I. Kondarides, Catal. Today 127 (2007) 319.
[30] A. Kotsifa, D.I. Kondarides, X.E. Verykios, Appl. Catal. B 72 (2007) 136.
[31] T.I. Halkides, D.I. Kondarides, X.E. Verykios, Appl. Catal. B 41 (2003) 415.
[32] M. Primet, J. Catal. 88 (1984) 273.
[33] K. Tanaka, J.M. White, J. Catal. 79 (1983) 81.
[34] G.S. Lane, E.E. Wolf, J. Catal. 105 (1987) 386.
[35] O.S. Alexeev, S.Y. Chin, M.H. Engelhard, L. Ortiz-Soto, M.D. Amiridis, J. Phys. Chem. B 109 (2005) 23430.
[36] A. Yee, S.J. Morrison, Hicham Idriss, J. Catal. 191 (2000) 30.
[37] F. Boccuzzi, A. Chiorino, M. Manzoli, D. Andreeva, T. Tabakova, J. Catal. 188 (1999) 176.
[38] P. Panagiotopoulou, J. Papavasiliou, G. Avgouropoulos, T. Ioannides, D.I. Kondarides, Chem. Eng. J. 134 (2007) 16.
[39] A. Bensalem, J.C. Muller, D. Tessier, F. Bozon-Verduraz, J. Chem. Soc. Faraday Trans. 92 (1996) 3233.
[40] R.A. Van Santen, J. Chem. Soc. Faraday Trans. I 83 (1987) 1915.
[41] B.L. Mojet, J.T. Miller, D.C. Koningsberger, J. Phys. Chem. B 103 (1999) 2724.
[42] G.S. Lane, J.T. Miller, F.S. Modica, M.K. Barr, J. Catal. 141 (1993) 465.
[43] P.A.J.M. Angevaare, H.A.C.M. Hendrickx, V. Ponec, J. Catal. 110 (1988) 18.
[44] S.D. Jackson, N.M. Glanville, J. Willis, G.D. McLellan, G. Webb, R.B. Moyes, S. Simpson, P.B. Wells, R. Whyman, J. Catal. 139 (1993) 207.
[45] H. Zhu, Z. Qin, W. Shan, W. Shen, J. Wang, J. Catal. 225 (2004) 267.
[46] D.E. Eastman, J.E. Demuth, H.M. Baker, J. Vac. Sci. Technol. 11 (1974) 273.
[47] T. Shido, Y. Iwasawa, J. Catal. 141 (1993) 71.
[48] G. Jacobs, L. Williams, U. Graham, D. Sparks, B.H. Davis, J. Phys. Chem. B 107 (2003) 10398.
[49] J.T. Miller, B.L. Meyers, F.S. Modica, G.S. Lane, M. Vaarkamp, D.C. Koningsberger, J. Catal. 143 (1993) 395.
[50] K. Christmann, G. Ertl, T. Pignet, Surf. Sci. 54 (1976) 365.
[51] K.E. Lu, R.R. Rye, J. Vac. Sci. Technol. 12 (1975) 334.
[52] K. Foger, J.R. Anderson, J. Catal. 54 (1978) 318.
[53] P.G. Menon, G.F. Froment, J. Catal. 59 (1979) 138.
[54] D.M. Stockwell, A. Bertucco, G.W. Coulson, C.O. Bennett, J. Catal. 113 (1988) 317.
[55] O. Alexeev, D.-W. Kim, G.W. Graham, M. Shelef, B.C. Gates, J. Catal. 185 (1999) 170.
[56] D.O. Uner, M. Pruski, T.S. King, J. Catal. 156 (1995) 60.
[57] F. Benseradj, F. Sadi, M. Chater, Appl. Catal. B 228 (2002) 135.
[58] D.I. Kondarides, X.E. Verykios, J. Catal. 174 (1998) 52.
[59] M.E. Dry, T. Shingles, L.J. Boshoff, G.J. Oosthuizen, J. Catal. 15 (1969) 190.
[60] G. Marcelin, J.E. Lester, S.F. Mitchell, J. Catal. 102 (1986) 240.
[61] B.W. Krupay, Y. Amenomiya, J. Catal. 67 (1981) 362.